Ab Initio and Kinetic Calculation for the Abstraction Reaction of Atomic O(^{3}P) with SiH_4

Qingzhu Zhang, Shaokun Wang, Jianhua Zhou, and Yueshu Gu*

School of Chemistry and Chemical Engineering, Shandong University, Jinan 250100, P. R. China

Received: July 16, 2001; In Final Form: October 2, 2001

The reaction of O(^{3}P) with silane was studied theoretically. The detailed mechanism was revealed for the first time. Two nearly degenerate transition states of ^{3}A″ and ^{3}A′ symmetries were located for the title reaction. Geometries were optimized at the UMP2 level with the 6-311G(2d,2p) basis set. The QCISD(T) level with the 6-311++G(3df,3pd) basis set was used in the final single-point energy calculations. On the basis of the ab initio data, the kinetic nature was studied using canonical variational transition-state theory (CVT) with small-curvature tunneling effect (SCT) correction. The rate constants were calculated over a wide temperature range of 200−3000 K. The CVT/SCT rate constants exhibit typical non-Arrhenius behavior, a three-parameter rate−temperature formula was fitted as follows: $k(T) = (1.53 \times 10^{-17})T^{2.25} \exp(-834.32/T)$ (in units of cm^3 molecule^{-1} s^{-1}). The calculated CVT/SCT rate constants match well with the experimental values.

1. Introduction

Silane is an important material in plasma chemical vapor deposition (CVD) and in semiconductor device process. The reaction of silane with O(^{3}P) is likely to be of considerable importance during the initial phase of plasma-enhanced and photoinduced chemical vapor deposition (CVD) of SiO_2 from SiH_4/N_2O mixtures and SiH_4/O_2 mixtures.[1−4] Modeling of the CVD mechanism requires kinetic information about the reaction of O(^{3}P) with silane.

Several experimental studies were reported on this reaction of O(^{3}P) with SiH_4. It can be seen from the early results published that there is a great disagreement about the mechanism of this reaction. Withnall and Andrews[5] proposed that this reaction proceeds via an insertion/addition mechanism forming a vibrationally excited silanol, which subsequently decomposes. However, the credibility of their interpretation is in doubt following their subsequent claim that O attack on the methylated silanes also proceeds via an insertion reaction. In a study of the vibrational and rotational distributions of the OH radical formed in the reaction of O with SiH_4, Wiesenfeld and his co-workers[6] argue that this reaction proceeds via a linear collision complex. However, they found that a small proportion of the OH radicals were rotationally excited, which led them to suggest that there is a minor contribution from an insertion reaction, which also results in the formation of OH radicals. Agrawalla and Setser[7] investigated the chemiluminescence and laser-induced fluorescence of OH radicals formed in the reaction of O(^{3}P) with SiH_4, and they[7] suggest that the dominant channel is the direct hydrogen abstraction. Another deficiency of the early studies is that the experimental rate constants are widely scattered, possibly as a result of the different experimental techniques employed. The Arrhenius expressions obtained by Atkinson[8] and Mkryan[9] are $k = 6.8 \times 10^{-12} \exp(-6.6\ \text{kJ/mol})/(RT)$ cm^3 molecule^{-1} s^{-1} over $T = 297-438$ K and $k = 2.7 \times 10^{-11} \exp(-11.3\ \text{kJ/mol})/(RT)$ cm^3 molecule^{-1} s^{-1} over $T = 280-549$ K. In an attempt to adjudicate between them and to obtain reliable rate constants, Horie[10] and Ding[11] studied this reaction successively, and they obtained satisfactory agreements. Both of them suggested that this reaction has a direct abstraction mechanism. In 1991, Horie investigated this reaction at room temperature in a discharge flow system with mass spectrometric detection and also in stationary photolysis experiments. Analysis of the end products provided conclusive evidence that the only primary process occurring in this reaction was the hydrogen abstraction from the Si−H bond by the O atom leading to the formation of the OH and silyl radicals. The value of the rate constant at 298 K obtained by him is 3.5×10^{-13} cm^3 molecule^{-1} s^{-1}, which is in good agreement with the value calculated from the Arrhenius expression of $k = 1.23 \times 10^{-10} \exp(-14.6\ \text{kJ/mol})/(RT)$ cm^3 molecule^{-1} s^{-1} fitted by Ding over the temperature range of 295−565 K.

However, the theoretical work is very limited for this reaction. To our knowledge, there is only one theoretical study about the reaction of O(^{3}P) with SiH_4. In 1993, Ding[11] studied the reaction using ab initio molecular orbital theory combined with the canonical transition state theory (TST).[12] The geometric parameters and frequencies were calculated at the HF/6-31G(d) and MP2/6-31G(d) levels, and the energies were calculated at the G2 level of theory.[13] A better value of the potential barrier obtained by him is 11.3 kJ/mol at P-G2//MP2/6-31G(d). On the basis of the ab initio data, the rate constants of the reaction of O(^{3}P) with SiH_4 were calculated over the temperature range of 295−2000 K, and a three-parameter rate−temperature expression was fitted as follows: $k_{TST} = (5.1 \times 10^{-17})T^{2.15} \exp(-1062/T)$ cm^3 molecule^{-1} s^{-1}, with a high degree of curvature in the rate−temperature plot. It is obvious that his study is rather rough. Another deficiency in his study is that he did not take into account the Jahn−Teller effect. For this H atom abstraction reaction, the approach of the O(^{3}P) to SiH_4 with C_s symmetry proceeds over two potential energy surfaces (PESs), $^3A' + {}^3A''$, generated by the Jahn−Teller effect. Indeed, for C_s symmetry the irreducible representation is $^3A' + {}^3A''$ for reactants and $^3A' + {}^3A'' + {}^3A' + {}^3A''$ for products, and therefore, both asymptotes adiabatically correlate through the PESs $^3A'$ and $^3A''$ in C_s. Unfortunately, only one transition state was located in the study of Ding. Therefore, the rate constants calculated by Ding are the values of one PES and not the overall rate constants of this reaction.

* To whom correspondence should be addressed. E-mail: guojz@icm.sdu.edu.cn.

10.1021/jp0127317 CCC: $22.00 © 2002 American Chemical Society
Published on Web 12/01/2001

In this paper, we first calculated geometrical parameters, frequencies, and energies of the reactant, transition states, and products for this hydrogen abstraction reaction. In a second step, we carried out the kinetic calculations using the canonical variational transition state theory (CVT)[14−16] with the small-curvature tunneling correction method (SCT).[17] Several features of this work are the following: (1) The reaction mechanism was revealed. This reaction proceeds via a direct hydrogen abstraction mechanism

$$O(^3P) + SiH_4 \rightarrow OH + SiH_3$$

which is different apparently from the insertion mechanism of the reactions of $O(^1D)$ with SiH_4. (2) Two nearly degenerate transition states of $^3A''$ and $^3A'$ symmetries were located. (3) The potential energy profile surface was calculated at the QCISD(T) level (a quadratic configuration interaction calculation including single and double substitutions with a triples contribution) with the 6-311++G(3df,3pd) basis set. (4) The rate constants were obtained over a wide temperature range of 200−3000 K, and the non-Arrhenius expression was fitted. (5) The calculated overall rate constants were compared with the available experimental values.

2. Computation Methods

Ab initio calculations were carried out using Gaussian 94 programs.[18] The geometries of the reactant, transition states, and products were optimized at the UMP2 level (second-order perturbation Moller−Plesset method) with the 6-311G(2d,2p) basis set. The vibrational frequencies were calculated at the same level of theory to determine the nature of different stationary points and the zero-point energy (ZPE). The intrinsic reaction coordinate (IRC)[19] calculation confirms that the transition state connects the designated reactants and products. At the UMP2/6-311G(2d,2p) level, the minimum energy path (MEP)[20] was obtained with a gradient step size of 0.05 $amu^{1/2}$ b in mass-weighted Cartesian coordinates. The force constant matrixes of the stationary and selected nonstationary points near the transition state along the MEP were also calculated.

Although the geometrical parameters and the frequencies of various species can be determined satisfactorily at the UMP2/6-311G(2d,2p) level, the energies obtained at this level may not be accurate enough for the subsequent kinetic calculations. Therefore, a higher level, QCISD(T), and a more flexible basis set, 6-311++G(3df,3pd), were employed to calculate the energies of various species.

The initial information obtained from our ab initio calculations allowed us to calculate the variational rate constants including the tunneling effect. The canonical variational theory (CVT) rate constant for temperature, T, is given by

$$k^{CVT}(T) = \min_s k^{GT}(T,s) \qquad (1)$$

where

$$k^{GT}(T,s) = \frac{\sigma k_B T}{h} \frac{Q^{GT}(T,s)}{\Phi^R(T)} e^{-V_{MEP}(s)/(k_B T)} \qquad (2)$$

where, $k^{GT}(T,s)$ is the generalized transition state theory rate constant at the dividing surface, s, σ is the symmetry factor accounting for the possibility of more than one symmetry-related reaction path, k_B is Boltzmann's constant, h is Planck's constant, $\Phi^R(T)$ is the reactant partition function per unit volume, excluding symmetry numbers for rotation, and $Q^{GT}(T,s)$ is the partition function of a generalized transition state at s with a local zero of energy at $V_{MEP}(s)$ and with all rotational symmetry numbers set to unity. The tunneling contribution was also considered. Only the centrifugal-dominant small-curvature tunneling (SCT) method was used. Methods for large-curvature cases have been developed, but they require more information about the PES than what was determined in the present study. All the kinetic calculations were carried out using the POLYRATE 7.8 program.[21]

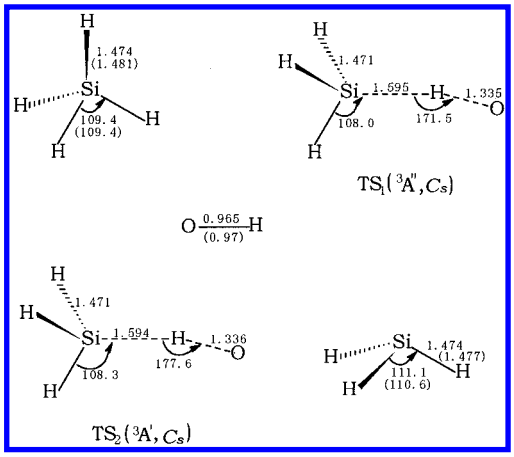

Figure 1. UMP2/6-311G(2d,2p) optimized geometries for stationary points. Distance is in Å, and angle is in deg. The values in parentheses are experimental data.[23]

TABLE 1: Vibrational Frequencies (in cm^{-1}) and Zero-Point Energies (ZPE, in kcal/mol) for the Reactant, Products, and Transition States Involved in the Reaction of $O(^3P)$ with SiH_4. The Values in Italics Are the Experimental Data[23]

species	frequencies									ZPE
SiH_4	966	966	966	1020	1020	2302	2302	2302	2302	20.22
	913	*913*	*913*	*972*	*972*	*2186*	*2189*	*2189*	*2189*	
SiH_3	813	978	978	2275	2303	2303				13.79
	773	*933*	*933*	*2150*	*2180*	*2180*				
OH	3833									5.48
TS($^3A''$)	1845i	118	242	507	873	894	927	987	991	17.84
	2304	2318	2320							
TS($^3A'$)	1842i	268i	239	500	870	927	950	977	995	
	2304	2348	2318							

TABLE 2: The Calculated Potential Barrier, ΔE, and the Reaction Enthalpy, ΔH, at Various Theory Levels Including the UMP2 ZPE Correction[a]

levels	ΔE			ΔH
	$^3A''$		$^3A'$	
MP2/6-311++G(3df,3pd)	6.17	*8.55*	*8.55*	−15.15
MP4/6-311++G(3df,3pd)	7.30	*9.68*	*9.69*	−10.95
QCISD(T)/6-311++G(3df,3pd)	2.83	*5.33*	*5.34*	−11.05
exptl				−11.09

[a]The values are in kcal/mol. The values in italics correspond to the energies without including the ZPE. The experimental value is obtained from ref 11.

3. Results and Discussion

The optimized geometries of the reactant, transition states, and products are shown in Figure 1. The vibrational frequencies and the zero-point energy (ZPE) of the reactant, products, and transition states are listed in Table 1. The potential barrier, ΔE, and the reaction enthalpy, ΔH, calculated are summarized in Table 2.

3.1. Reaction Mechanism. It is worth stating the reliability of the calculations in this work. Because unrestricted Hartree−

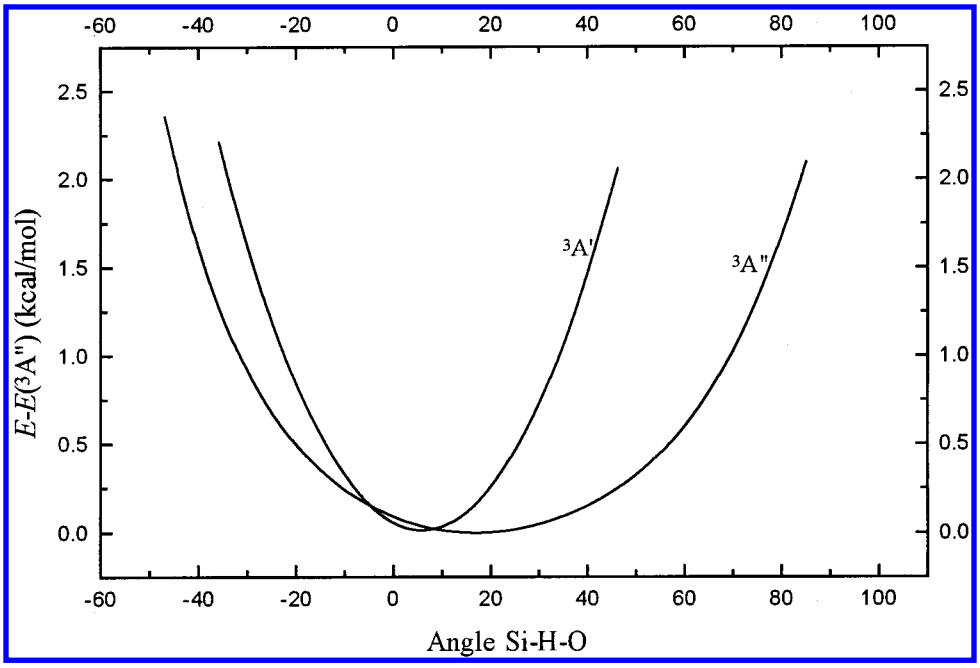

Figure 2. Energy profile for the ^{3}A′ and ^{3}A″ potential energy curves with respect to their minima at the UMP2/6-311G(2d,2p) level. For these calculations, the other internal coordinates were fixed at their respective values in the minimum. The zero value on the *x*-axis corresponds to the Si−H−O angle of the ^{3}A″ transition state.

Fock (UHF) reference wave functions are not spin eigenfunctions for open-shell species, we monitored the expectation values of $\langle S^2 \rangle$ in the UMP2/6-311G(2d,2p) optimization. The values of $\langle S^2 \rangle$ are always in the range of 0.750−0.757 for doublets and in the range of 2.000−2.036 for triplets. After spin annihilation, the values of $\langle S^2 \rangle$ are 0.750 for doublets and 2.000 for triplets, where 0.750 and 2.000 are the exact values for a pure doublet and for a pure triplet. Thus, spin contamination is not severe. This suggests that a single determinant reference wave function for this system is suitable for the level of theory used in the optimization.[22]

a. Geometry and Frequency. To clarify the general reliability of the theoretical calculations, it is useful to compare the predicated chemical properties of the present particular systems of interest with experimental data. As shown in Figure 1, the geometric parameters of SiH_4, SiH_3, and OH are in good agreement with the available experimental values. From this result, it might be inferred that the same accuracy could be expected for the calculated transition-state geometries. As can be seen from Table 1, the vibrational frequencies of both the reactant and the products agree well with the experimentally observed fundamentals, and the relative error is less than 6%.

Next, we consider the transition states, for which we performed a more detailed analysis. At first, we attempted to find a transition state using a Z-matrix having an initial value of 180.0° for the angle Si−H−O, but the optimization always produced a new value of 171.5°, which corresponds to ^{3}A″ symmetry. In other words, we could not find a transition state with C_{3V} symmetry, having a linear fragment. This means that the O(^{3}P) atom approaches the SiH_4 with C_s symmetry. In this case, according to the Jahn−Teller effect theorem, this abstraction reaction actually proceeds on two potential energy surfaces with ^{3}A″ and ^{3}A′ symmetries.

At the UMP2/6-311G(2d,2p) level, two transition states with ^{3}A″ and ^{3}A′ symmetry were located, the geometrical structures of which are shown in Figure 1. Population analysis shows that the half-filled p orbital of the ^{3}A″ symmetry is in the HSiHO plane and the half-filled p orbital of the ^{3}A′ symmetry is perpendicular to this plane. In the present work, we found that the ^{3}A″ and ^{3}A′ transition states were almost identical in energy but differ slightly in the Si−H−O bending angle. The Si−H−O angle is 171.5° for the transition state with ^{3}A″ symmetry, while this angle is 177.6° for the one with ^{3}A′ symmetry. Therefore, the ^{3}A″ transition state is more "bent" than the ^{3}A′ one. The breaking Si−H bonds are elongated by 8.2% and 8.1%, while the forming O−H bonds are longer than the equilibrium value of 0.965 Å by 38.3% and 38.4% for the transition states of ^{3}A″ and ^{3}A′, respectively. Therefore, these two transition states are reactant-like, and the H abstraction reaction from SiH_4 by O atom proceeds via early transition states. This rather early character in these transition states is in accordance with the low reaction barrier and the high exothermicity of this reaction, in keeping with Hammond's postulate.

As shown in Table 1, at the UMP2/6-311G(2d,2p) level, the ^{3}A″ transition state has only one imaginary frequency (1845i cm^{-1}); however, for the ^{3}A′ case two imaginary frequencies are present with values of 1842i and 268i cm^{-1}. A UB3LYP/6-311G(d,p) calculation also yields two imaginary frequencies for the ^{3}A′ transition state. We were unable to determine a ^{3}A′ transition state with a single imaginary frequency. The smaller imaginary frequency is regarded as a hindered internal rotation. Similar results were found in two studies: Kreye[24] in a study of the reaction of O(^{3}P) with CHF_3 at UMP2/6-311G(d,p) located a transition state on the ^{3}A′ surface with two imaginary frequencies (2645i and 87i cm^{-1}); Gonzalez[25] determined a ^{3}A′ transition state with two imaginary frequencies (2258.1i and 173.5i) for the reaction of O(^{3}P) with CH_4 at UMP2/6-311G-(3d2f,3p2d) level.

To get a clearer view of the ^{3}A″ and ^{3}A′ surfaces, we have carried out electron calculations at the UMP2/6-311G(2d,2p) level, varying the angle Si−H−O in relation to its respective optimized transition state geometry. Figure 2 shows the calculations of the PESs in C_s symmetry, where all values (angles and energies) are referred to the most stable ^{3}A″ structure and the internuclear distances, *d*(Si−H) and *d*(H−O), are fixed. The calculated PES is very flat, and in the region of +10° to −15°, the difference in energy between the ^{3}A″ and ^{3}A′ electronic PES is less than 0.1 kcal/mol.

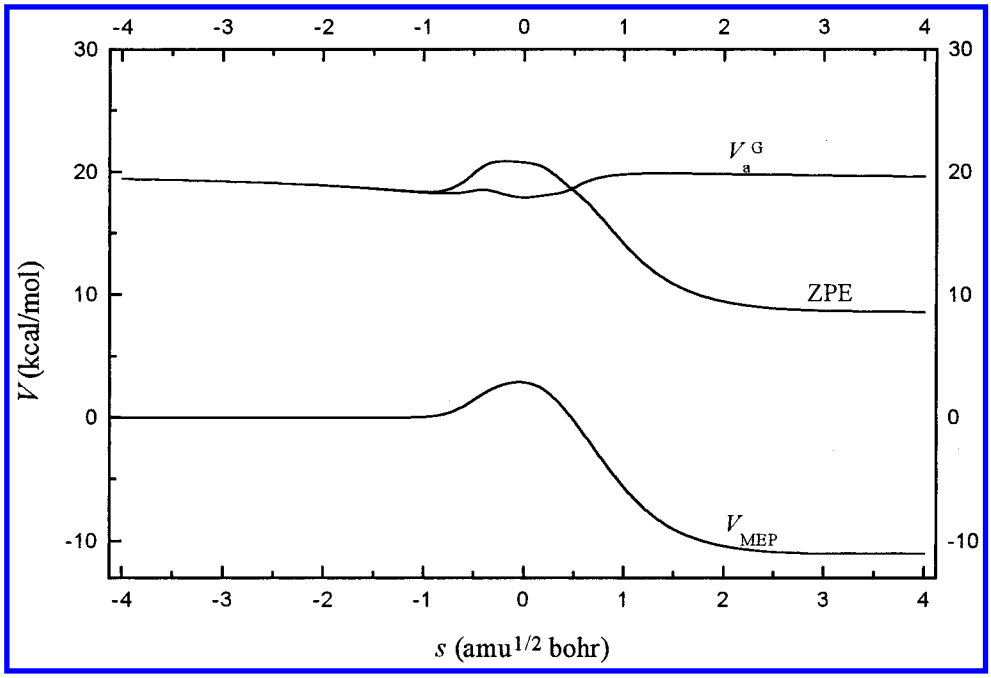

Figure 3. The potential energy (V_{MEP}) and vibrationally adiabatic potential energy curves (V_a^G) as functions of s at the QCISD(T)/6-311++G-(3df,3pd) level for the $^3A''$ potential energy surface.

To confirm further that these two transition states of $^3A''$ and $^3A'$ connect the designated reactants and products, with a step size of 0.05 amu$^{1/2}$ b, the intrinsic reaction coordinate (IRC) was calculated at the UMP2/6-311G(2d,2p) level from the transition states to the reactants and the products. For these two transition states, $^3A''$ and $^3A'$, the changing curves of the bond lengths are almost overlapping. The breaking bond, Si−H, is almost unchanged from $s = -\infty$ to $s = -0.3$ amu$^{1/2}$ b and equals the value of the reactant and stretches after $s = -0.3$ amu$^{-1/2}$ b. The forming H−O bond shortens rapidly from reactants and reaches the equilibrium bond length of OH at $s = 0.7$ amu$^{1/2}$ b. Other bond lengths are almost unchanged during the reaction process. Therefore, both transition states of $^3A''$ and $^3A'$ connect the reactants (SiH_4 and O) with the products (SiH_3 and OH). The geometric changes mainly take place in the region from $s = -0.3$ to $s = 0.7$ amu$^{1/2}$ b.

b. Energy. Table 2 summarizes the potential barrier, ΔE, and the reaction enthalpy, ΔH, relative to the reactants at various theory levels. First, we analyze the reaction enthalpy. Ding obtained a better experimental value of −11.09 kcal/mol from the measured $\Delta H_{f,298}(SiH_3)$ together with $H_{298}-H_0(SiH_3)$ calculated by Hudgens and $\Delta H_{f,0}$ for O, SiH_4, and OH. The values of −15.15 kcal/mol calculated the MP2 level with 6-311++G-(3df,3pd) are in great disagreement with the experimental values (−11.09 kcal/mol); similar calculations using the same basis set with the highly correlated and more computationally demanding MP4 and QCISD(T) level predict the values of −10.95 and −11.05 kcal/mol, in excellent agreement with the experimental value. These results clearly indicated that most of the error in the reaction enthalpy computed at MP2 with the 6-311++G(3df,3pd) basis set can be attributed to the lack of correlation in such a method and not to an improper optimized geometry at UMP2/6-311G(2d,2p).

With respect to the potential barrier, the values without ZPE correction are almost identical for the two potential energy surfaces of $^3A''$ and $^3A'$ at the same level. This means that the two transition states are almost identical in energy. However, the values for the same potential energy surface have a great discrepancy obtained at the MP2, MP4, and QCISD(T) levels. Taking into account the calculated results of the reaction enthalpy at these levels, we think that the result calculated at the QCISD(T) level with 6-311++G(3df,3pd) is the most reliable, and the MP2 and MP4 levels yield a strong overestimate for the potential barrier. Therefore, the energies calculated at QCISD(T)/6-311++G(3df,3pd) level are used for the kinetic calculation.

The similarity of the two transition states in the geometries and frequencies allows us to assume that the dynamics for both $^3A''$ and $^3A'$ surfaces will be very similar. Thus, we calculate the rate constant for the whole reaction as twice the rate constant for one of the surfaces. The same method of treatment has been successfully used to calculate the rate constants of the reactions of O(^{3}P) with CHF_3 and CH_4 by Kreye[24] and Gonzalez.[25] In particular, we calculate the rate constants for the $^3A''$ surface, and we multiply them by 2 to obtain the rate constants for the reaction of O(^{3}P) with SiH_4. Therefore, we mainly discuss the kinetic calculation on the $^3A''$ surface in the following study.

3.2. The Kinetic Calculation. *a. Reaction Path Properties.* The minimum energy path (MEP) was calculated at the UMP2/6-311G(2d,2p) level by the IRC theory, and the energies of the MEP were refined by the QCISD(T)//UMP2 method. The maximum position of the classical potential energy curve, V_{MEP}, at the QCISD(T)/6-311++G(3df,3pd)//UMP2/6-311G(2d,2p) level corresponds to the saddle point structure at the UMP2/6-311G(2d,2p) level. Therefore, the shifting of the maximum position for the V_{MEP} curve caused by the computational technique is avoided. The changes of the classical potential energy, V_{MEP}, and the ground-state vibrational adiabatic potential energy, V_a^G, with the reaction coordinate s are shown in Figure 3. It can be seen that the maximum positions of the V_{MEP} and V_a^G energy curves are different at the QCISD(T)//UMP2 level. The maximum positions of V_a^G ($s = -0.32$ amu$^{1/2}$ b) deviate from the position of the saddle point ($s = 0.0$ amu$^{1/2}$ b). This means that the variational effect will be significant for the calculation of the rate constants. The zero-point energy, ZPE, which is the difference between V_a^G and V_{MEP}, is also shown in Figure 3. The zero-point energy curve is almost unchanged as

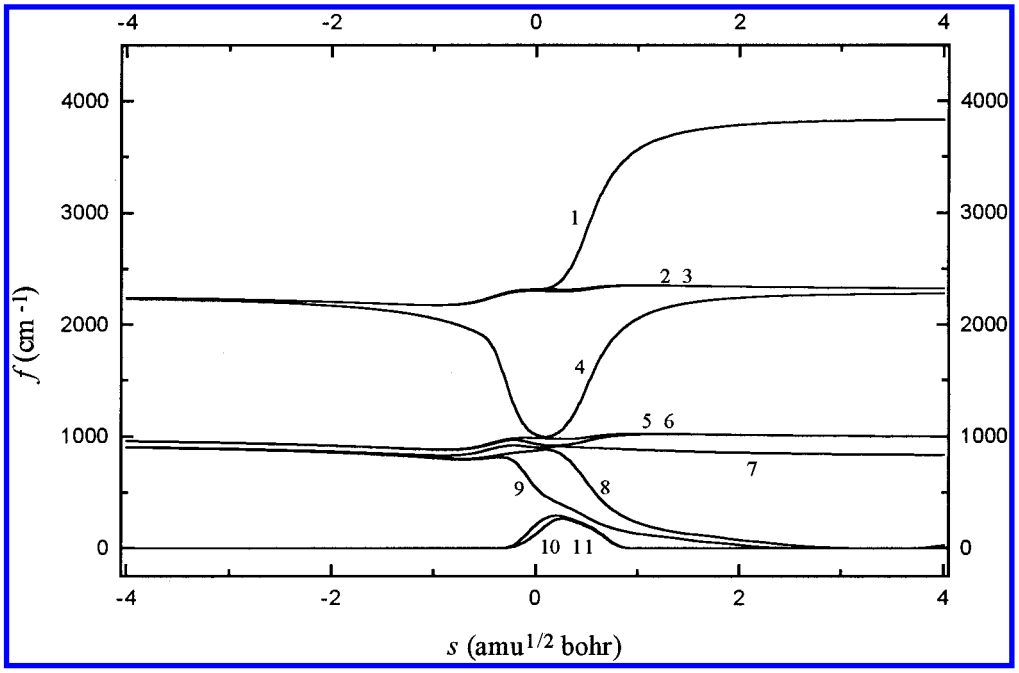

Figure 4. Changes of the generalized normal-mode vibrational frequencies as functions of *s* at the UMP2/6-311G(2d,2p) for the ^{3}A″ potential energy surface.

s varies except that only from $s = -0.5$ to 0.5 amu$^{1/2}$ b there is a gentle drop. To analyze this behavior in greater detail, we show the variation of the generalized normal modes vibrational frequencies on the ^{3}A″ potential surface in Figure 4.

In the negative limit of *s*, the frequencies are associated with the reactants, while in the positive limit of *s*, the frequencies are associated with the products. For the sake of clarity, the vibrational frequencies can be divided into three types: spectator modes, transitional modes, and reactive modes. The spectator modes are those that undergo little change and sometimes remain basically unchanged in going from reactants to the transition state. The transitional modes appear along the reaction path as a consequence of the transformation from free rotation or free translations within the reactant or the product limit into real vibrational motions in the global system. Their frequencies tend to zero at the reactant and the product limit and reach their maximum in the saddle-point zone. The reactive modes are those that undergo the largest change in the saddle-point zone, and therefore, they must be related to the breaking/forming bonds. For the reaction of O(^{3}P) with SiH_4, mode 4, which connects the frequency of the Si−H stretching vibration of SiH_4 with the frequency of the O−H stretching vibration of OH, is the reactive mode, modes 10 and 11 are transitional modes, and other modes are spectator modes. From $s = -0.5$ to $s = 0.5$ amu$^{1/2}$ b, the reactive modes drop dramatically; this behavior is similar to that found in other hydrogen abstraction reactions.[26−28] A priori, this drop should cause a considerable fall in the zero-point energy near the transition state. But because this kind of drop of the reactive mode is compensated partially by the transitional modes, the drop of the zero-point energy in the saddle zone is gentle.

b. The Rate Constant. The canonical variational transition state theory (CVT) with a small-curvature tunneling correction (SCT), which has been successfully performed for several analogous reactions, is an effective method to calculate the rate constants. In this paper, we used this method to calculate the rate constants of the reactions of O atom with SiH_4 over a wide temperature range from 200 to 3000 K.

To calculate the rate constants, 30 points were selected near the transition state region along the MEP, 15 points in the reactant zone and 15 points in the product zone. The canonical variational transition state theory (CVT) is based on the idea of varying the dividing surface along a reference path to minimize the rate constant, and thermodynamically minimizing the rate constant is equivalent to maximizing the standard-state free energy change, $\Delta G(T,s)$, so the variational effect can be shown by the maximum position of $\Delta G(T,s)$. The maximum positions of $\Delta G(T,s)$ on the ^{3}A″ potential surface are from $s = -0.1$ to -0.32 amu$^{1/2}$ b over the temperature range of 200−3000 K. Thus, the variation effects, that is, the ratio between variational CVT and conventional TST rate constants, are great. Therefore, for this reaction, not only the energy contribution but also the entropy contribution should be taken into account in the calculation of the rate constant.

Figure 5 shows the calculated CVT rate constants, the CVT/SCT rate constants (as twice the rate constants of the ^{3}A″ surface), and the experimental values against the reciprocal of the temperature for the reaction of O(^{3}P) with SiH_4. For the purpose of comparison, the conventional transition state theory (TST) rate constants (as twice the TST rate constants of the ^{3}A″ surface) are also shown in Figure 5. Several features of the calculated rate constants are the following:

(1) It is seen that the TST rate constants are much greater than the CVT values, which enables us to conclude that the variational effects are significant to the calculation of the rate constant. This is in accordance with the above analysis.

(2) The quantum tunneling effect, which is the ratio between the CVT/SCT rate constants and CVT rate constants, is also significant for this reaction. For example, at 298 K, the CVT rate constant is 7.85×10^{-14} cm^3 molecule^{-1} s^{-1}, while the CVT/SCT rate constant is 3.43×10^{-13} cm^3 molecule^{-1} s^{-1}. The latter is 4.37 times larger than the former. Even at high temperature, the tunneling effect cannot be negligible.

(3) By comparison of the calculated rate constants with the experimental values of Ding[11] for the title reaction, it can be seen that the CVT/SCT rate constants are in good agreement with the experimental values over the temperature range of 295−565 K. From this result, it might be inferred that the same accuracy could be expected for the values over other temperature ranges. Therefore, the CVT/SCT method is a good choice to

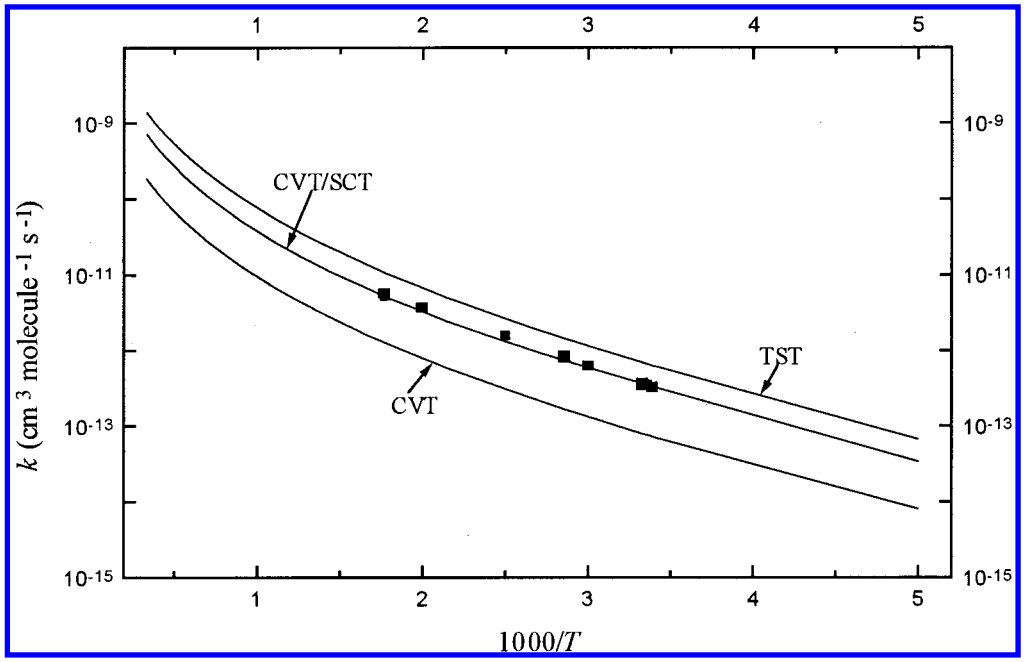

Figure 5. Rate constants as functions of the reciprocal of the temperature (K) in the temperature range 200−3000 K for the whole reaction of H with SiH_4. The ■ symbols are the experimental values obtained from the Arrhenius expression fitted by Ding.

calculate accurate rate constants for the title system. This good agreement testifies that the hydrogen abstraction mechanism is reasonable for the reaction of $O(^3P)$ with SiH_4. We cannot find the insertion products, such as $^3SiH_3OH$. Therefore, there is no theoretical evidence for the insertion mechanism. The TST method overestimates rate constants, while the CVT method underestimates rate constants.

(4) It is obvious that the calculated rate constants exhibit typical non-Arrhenius behavior. The rate constants of the title reaction are fitted by a three-parameter formula over the temperature range of 200−3000 K and given in units of cm^3 $molecule^{-1}$ s^{-1} as follows:

$$k(T) = (5.52 \times 10^{-17})T^{2.17} \exp(-890.48/T),$$
for TST rate constants

$$k(T) = (3.45 \times 10^{-18})T^{2.27} \exp(-864.25/T),$$
for CVT rate constants

$$k(T) = (1.53 \times 10^{-17})T^{2.25} \exp(-834.32/T),$$
for CVT/SCT rate constants

It is interesting to compare our study on this title reaction with the study of Ding.[11] The TST rate constants calculated by Ding are in excellent agreement with his experimental values. We think that the experimental study of Ding is very well executed, but there are several deficiencies existing in his theoretical study. (1) The Jahn−Teller effect has not been taken into account, and only one potential surface has been studied. (2) The variational effect has not been taken into account. (3) The imaginary frequency of the $^3A''$ transition state that we calculated is 1845i. The imaginary frequency calculated by Ding is 1985i at MP2/6-31G(d) and 2355i at HF/6-31G(d). The value of the imaginary frequency is very great. Therefore, the tunneling effect must be significant. However, there is no tunneling effect correction in the calculation of the rate constants of Ding. We think that the excellent agreement between the experimental values of Ding with his nonvariational TST without tunneling correction is probably due to error compensation. It is well-known that the nonvariational TST method overestimates the rate constant (the upper limit). Thus, the overestimation of the TST method compensates for the lack of one potential surface. Our TST rate constants (as twice the TST rate constants of the $^3A''$ surface) should be two times the TST values (the values of only one PES) of Ding. At 298 K, the TST rate constant of Ding is 3.02×10^{-13} cm^3 $molecule^{-1}$ s^{-1}, while half of our TST value is 3.25×10^{-13} cm^3 $molecule^{-1}$ s^{-1}. At 1000 K, the TST rate constant of Ding is 4.97×10^{-11} cm^3 $molecule^{-1}$ s^{-1}, while half of our TST value is 3.67×10^{-13} cm^3 $molecule^{-1}$ s^{-1}.

4. Conclusion

In this paper, we studied the reaction of $O(^3P)$ with SiH_4 using ab initio and canonical variational transition state theory (CVT) with the small-curvature tunneling effect. Rate constants were reported over the temperature range of 200−3000 K. Several major conclusions can be drawn from this calculation.

1. This reaction proceeds via a direct hydrogen abstraction mechanism.

2. For this H atom abstraction reaction, the approach of the $O(^3P)$ to SiH_4 with C_s symmetry proceeds over two potential energy surfaces (PESs), $^3A' + {}^3A''$, generated by the Jahn−Teller effect.

3. The $^3A'$ transition state has two imaginary frequencies. The rate constants for the whole reaction are twice the rate constants of the $^3A''$ surface.

4. The calculated rate constants exhibit typical non-Arrhenius behavior.

Acknowledgment. The authors thank Professor Donald G. Truhlar for providing the POLYRATE 7.8 program. This work is supported by the Research Fund for the Doctoral Program of Higher Education of China.

References and Notes

(1) Giunta, C. J.; Chapple-Sokol, J. D.; Gordon, R. G. *J. Electrochem. Soc*. **1990**, *137*, 3237.

(2) Bhatnagar, Y. K.; Milne, W. I. *Thin Solid Films* **1989**, *168*, 345.

(3) Chapple-Sokol, J. D.; Giunta, C. J.; Gordon, R. G. *J. Electrochem. Soc*. **1989**, *136*, 2993.

(4) Liehr, M.; Cohen, S. A. *Appl. Phys. Lett.* **1992**, *60*, 198.
(5) Withnall, R.; Andrews, L. *J. Phys. Chem.* **1985**, *89*, 3251.
(6) Park, C. R.; White, G. D.; Wiesenfeld, J. R. *J. Phys. Chem*. **1988**, *92*, 152.
(7) Agrawalla, B. S.; Setser, D. W. *J. Chem. Phys*. **1987**, *86*, 5421.
(8) Atkinson, R.; Pitts, J. N., Jr. *Int. J. Chem. Kinet*. **1978**, *10*, 1151.
(9) Kharutunyan, S. A.; Mkryan, T. G.; Sarkisyan, E. N. *Oxid. Commun.* **1984**, *7*, 49.
(10) Horie, O.; Taege, R.; Reimann, B.; Arthur, N. L.; Potzinger, P. *J. Phys. Chem*. **1991**, *95*, 4393.
(11) Ding, L.; Marshall, P. *J. Chem. Phys*. **1993**, *98* (11), 8545.
(12) Laidler, K. J. *Chemical Kinetics*, 3rd ed.; Harper and Row: New York, 1987.
(13) Curtiss, L. A.; Raghavachavi, K.; Trucks, G. W.; Pople, J. A. *J. Chem. Phys*. **1991**, *94*, 7221.
(14) Baldrige, K. K.; Gordor, M. S.; Steckler, R.; et al. *J. Phys. Chem*. **1989**, *93*, 5107.
(15) Gonzalez-Lafont, A.; Truong, T. N.; Truhlar, D. G. *J. Chem. Phys*. **1991**, *95* (12), 8875.
(16) Garrett, B. C.; Truhlar, D. G. *J. Phys. Chem.* **1979**, *83* (8), 1052.
(17) Liu, Y. P.; Lynch, G. C.; Truong, T. N.; Lu, D. H.; Truhlar, D. G. *J. Am. Chem. Soc*. **1993**, *115*, 2408.
(18) Frisch, M. J.; Trucks, G. W.; Schlegel, H. B.; Gill, P. M. W.; Johnson, B. G.; Robb, M. A.; Cheeseman, J. R.; Keith, T.; Petersson, G. A.; Montgomery, J. A.; Raghavachari, K.; Al-Laham, M. A.; Zakrzewski, V. G.; Ortiz, J. V.; Foresman, J. B.; Cioslowski, J.; Stefanov, B. B.; Nanayakkara, A.; Challacombe, M.; Peng, C. Y.; Ayala, P. Y.; Chen, W.; Wong, M. W.; Andres, J. L.; Replogle, E. S.; Gomperts, R.; Martin, R. L.; Fox, D. J.; Binkley, J. S.; Defrees, D. J.; Baker, J.; Stewart, J. P.; Head-Gordon, M.; Gonzalez, C.; Pople, J. A. *Gaussian 94*, revision E.1; Gaussian, Inc.: Pittsburgh, PA, 1995.
(19) Garrett, B. C.; Truhlar, D. G. *J. Phys. Chem*. **1983**, *87*, 4553.
(20) Garrett, B. C.; Truhlar, D. G. *J. Phys. Chem*. **1979**, *83*, 1079.
(21) Steckler, R.; Chuang, Y. Y.; Fast, P. L.; Corchade, J. C.; Coitino, E. L.; Hu, W. P.; Lynch, G. C.; Nguyen, K.; Jackells, C. F.; Gu, M. Z.; Rossi, I.; Clayton, S.; Melissas, V.; Garrett, B. C.; Isaacson, A. D.; Truhlar, D. G. *POLYRATE Version*; University of Minnesota: Minneapolis, MN, 1997.
(22) Liu, R.; Francisco, J. S. *J. Phys. Chem. A* **1998**, *102*, 9869.
(23) Espinosa-Garcia, J.; Sanson, J.; Corchado, J. C. *J. Chem. Phys*. **1998**, *109* (2), 466.
(24) Kreye, W. C. *Chem. Phys. Lett.* **1996**, *256*, 383.
(25) Gonzalez, M.; Hernando, J.; Millan, J.; Sayos, R. *J. Chem. Phys*. **1999**, *110* (15), 7326.
(26) Espinosa-Garcia, J.; Corchado, J. C. *J. Phys. Chem.* **1996**, *100*, 16561.
(27) Corchado, J. C.; Espinosa-Garcia, J. *J. Chem. Phys.* **1997**, *106*, 4013.
(28) Espinosa-Garcia, J.; Corchado, J. C. *J. Phys. Chem.* **1997**, *101*, 7336.